The typical permissible overspeed limit is about 5–7% of design mechanical speed. Thus fan-corrected speed needs to be reduced if its mechanical speed exceeds the limiting value. It will alter the engine steady-state performance, and the optimum system definition as obtained earlier will also change.

To investigate this issue, another optimization study was performed in which the fan mechanical speed was limited to 1.07 times its design speed. It results in W_{TO} and $W_{ENG,SLS}$ that are of the same order of magnitude as at the conventional design point.

As design Mach number increases at $H = 9.0$ km., optimum TR begins to decrease. This is because the increase in design Mach number causes the $T_{1,DP}$ and, hence, TET_{DP} also to increase, which reduces TR. There is a flight point, which is $M = 1.55$ in the present case, at which TR equals 1.0. If a higher Mach number, e.g., 1.60, is chosen as the design point, the optimum value of W_{TO} begins to increase because the least value that TR can take is 1.0. Thus as design Mach number increases, TET_{max} occurs at a higher Mach number (or $T_{1,DP}$), and the engine operates at relatively reduced TET at a large number of flight points, where Mach number (or T_1) is lower than that of the design point.

Though not investigated, the trends as observed at design altitude of 9.0 km should also hold true at other design altitudes, because any design combination of H/M can be translated into an equivalent $T_{1,DP}$, which then dictates the quality of chosen flight point as the engine design point. As a typical example, cycle optimization results at $H = 6.0$ km/$M = 1.3$ in ISA at $DT_{amb} = 0$ K ($T_{1,DP} = 333$ K) are not significantly different in comparison to that at $H = 9.0$ km/$M = 1.5$ in ISA at $DT_{amb} = 0$ K, which also corresponds to $T_{1,DP} = 333$ K.

To summarize, at a prescribed design altitude there is a lower limit on $T_{1,DP}$, below which (despite a lower value of optimum W_{TO}) the resulting cycle is not practically feasible. There also exists an upper limit on $T_{1,DP}$ beyond which cycle optimization results in an increased optimum W_{TO}. Between these limits of $T_{1,DP}$, cycle optimization, results do not differ significantly within themselves and in comparison with that at the conventional design point. Thus instead of searching for an optimum design point, it is sufficient to perform conceptual design system optimization at the conventional engine design point.

Conclusions

The value that $T_{1,DP}$ takes at an H/M combination dictates its suitability as the engine design point. If minimization of W_{TO} is the criteria for engine cycle optimization, then a flight condition with a low $T_{1,DP}$ is more suited as the design point because it results in a lower value of optimum W_{TO}. However, it also requires the engine to overspeed continuously for long durations, thereby causing an increased engine weight and reduction in the life of the rotating components. If this overspeeding is restricted to the current design limits of about 7% of design speed, savings in W_{TO} diminish.

As $T_{1,DP}$ increases, there arises a flight point at which TR equals 1.0. Because TR cannot take a value lower than 1.0, choosing further higher values of $T_{1,DP}$ only delays the occurrence of TET_{max}. There will be a large number of flight points at which T_1 is lower than $T_{1,DP}$. At all such points, the engine will operate at relatively lower values of TET, causing a penalty in the optimum W_{TO}.

Between these lower and upper ranges of $T_{1,DP}$, there is no significant difference in cycle optimization results, and it is practically independent of design point choice. Thus the use of conventional engine design point itself is adequate for conceptual design cycle optimization.

References

[1]Sanghi, V., "Computer Aided Conceptual Design of Propulsion System for Combat Aircraft," Ph.D. Dissertation, Dept. of Aerospace Engineering, Indian Inst. of Technology, Bombay, India, 1996.

[2]Sanghi, V., Kishore Kumar, S., Sundararajan, V., and Sane, S. K., "Engine-Airframe Integration During Conceptual Design for Military Application," *Journal of Aircraft*, Vol. 35, No. 3, 1998, pp. 380–386.

[3]Mattingly, J. D., Heiser, W. H., and Daley, D. H., *Aircraft Engine Design*, AIAA Education Series, AIAA, New York, 1987.

Evaluation of Fuel Distribution in a Gas-Turbine Premixer: Influence of Swirl

A. R. Eaton,* S. F. Frey,* D. M. Cusano,*
M. W. Plesniak,† and P. E. Sojka‡
Purdue University, West Lafayette, Indiana 47907-1003

I. Introduction

MORE stringent regulations are requiring gas turbine manufacturers to reduce NO_x emissions. One method is to control the flame zone temperature through lean combustion. Thorough mixing of air and fuel is essential for minimal emissions. Hence, studies must be performed to understand how design parameters influence mixing characteristics.

Several methods are available to increase fuel–air mixing prior to combustion. The introduction of swirl is a common one because the fuel–air interaction time in the premixer is increased, and mixing enhanced, for a swirling flow. The enhancement in mixing is due in part to an increase in turbulence production and transport that results from straining of the flow.

Swirl also benefits the very lean operating conditions of these premixers by creating a recirculation zone in the combustion chamber that enhances flame stability. This flow reversal occurs for swirl number values greater than 0.5 (Ref. 1) and improves the combustion process by entraining and recirculating a portion of the hot combustion products, which in turn mix with and ignite the incoming fuel–air mixture. (In all cases, the swirl number is defined as $S = U/W = \tan\theta$, where U and W are the axial and tangential velocity components and θ is the premixer swirl vane angle.) This helps to not only stabilize the flame, but also to improve combustion efficiency, provide better flame blowoff limits, and reduce formation of gaseous and particulate pollutants.[2]

Several studies on normal jets issuing into swirling crossflows (a configuration representative of radial spray bars in an axisymmetric swirling flow) have been performed to better understand premixer flow characteristics. Ferrell et al.[3] and Ong et al.[4] reported results from extensive flow visualization studies on normal jets in swirling crossflows. Swirl numbers of 0, 1, and 2.75 (corresponding to swirl angles θ of 0, 45, and 70 deg) were examined under jet-to-crossflow momentum ratios of 2, 4, and 6. They showed that jet penetration decreased with an increase in swirl number because the bending of the jet was more pronounced at higher swirl numbers.

The experiments of Ahmed and So[5] confirmed that swirl has a dramatic effect on jet penetration. They used a one-component laser Doppler velocimeter to examine a jet in swirling crossflow (swirl number 2.25) with momentum ratios of 0.46 and 0.96. Jet penetration was found to increase with increased momentum ratio. The mean and turbulent velocity disturbances were also found to dissipate quickly. They concluded that a substantial fraction of the jet mean kinetic energy is converted into turbulent energy very rapidly, thus creating a high level of turbulence in the vicinity of the jet. This was found to improve mixing.

Chao and Ho[6,7] used a computational model to numerically study the mixing of a normal jet in a swirling crossflow. Comparisons of

Received 16 July 1998; revision received 11 December 1998; accepted for publication 3 February 1999.

*Graduate Research Assistant, Thermal Sciences and Propulsion Center, School of Mechanical Engineering.

†Associate Professor, Thermal Sciences and Propulsion Center, School of Mechanical Engineering; plesniak@ecn.purdue.edu. Senior Member AIAA.

‡Associate Professor, Thermal Sciences and Propulsion Center, School of Mechanical Engineering.

their predictions with the experimental results of Ferrell et al.,[3] Ong et al.,[4] and Lilley[8] led to the following conclusions: 1) The jet trajectory is dependent not only on the momentum ratio, but also on the strength (or swirl number) of the swirling crossflow and the jet-to-crossflow density ratio (which is mass or temperature related). 2) Heavier jets with a higher density ratio spread faster than lighter ones due to the deeper penetration of the jet. 3) Because of the pressure gradients developed in the swirling flow, the jet spreading is confined to the outer layer such that radial diffusion into the central vortex core is limited to only a minor amount of molecular diffusion in the near-field region of the jet (several jet diameters downstream of the injection point).

These previous studies can be summarized by noting that jets in crossflow exhibit decreased penetration with decreased momentum ratio and decreased penetration with increased swirl. In addition, jet mixing is confined to an outer ring for several jet diameters downstream of the injection point due to the pressure gradients developed in the swirling flow. Optimum mixing, based on the literature,[3] appears to be obtained at a swirl angle of 45 deg and a jet-to-crossflow momentum ratio of about 5. In addition, the effects of swirl configuration on vane swirler performance have been studied, e.g., by Lilley,[9] in an idealized configuration in which the low-speed velocity field was mapped.

The current study differs from previous investigations in that an actual piece of production hardware with practical fuel and air mass flow rates was used (totaling 150 g/s, or 0.33 lbm/s). Only two extreme cases were considered, no swirl and 48 deg of swirl (corresponding to a swirl number of 1.1), because of the expense of fabricating production-scale hardware. Although swirl is commonly used to stabilize the flame and prevent flashback into the mixer, its effects on mixing and, therefore, pollutant emissions have not been widely studied. The goals of the current experimental investigation then were twofold: to establish a baseline by investigating the level of mixedness for a representative gas turbine swirler–mixer and also to evaluate the effect of removing premixer swirl on air–fuel mixing.

II. Experimental Apparatus

The premixer–swirler studied is shown schematically in Fig. 1a. It is a multivaned axial unit that has an axisymmetric annular airflow passage into which extend a number of radially-directed fuel spray tubes. Each fuel spray tube has two sets of fuel delivery orifices; one is oriented tangent to the swirling air motion and the other downstream along the swirler axis, as shown in Fig. 1b.

Controlled quantities of air and fuel are supplied to the swirler. The simulated fuel was air seeded with Al_2O_3 particles having a diameter of approximately 1 μm to distinguish between the oxidizer air and the fuel air. A reverse cyclone seeder[10] was used to seed the fuel stream. Extinction measurements were performed to optimize seeder performance.[11]

Scalar concentration data at the premixer exit plane were obtained by using a Mie-scattering-based planar imaging system that consisted of a ruby laser, laser sheet forming/positioning optics, two charge-coupled device (CCD) cameras, and two personal computers with frame grabber boards. Image processing software consisted of commercial frame grabbing software (Data Translation's Global Lab Image) and Fortran code written specifically for this study. The measurement technique is described by Eaton et al.[11] The experimental apparatus is discussed in detail by Frey[12] and Eaton.[13] These authors also provide details of an uncertainty analysis performed on this system, which showed that the overall uncertainty (95% confidence) in the reported fuel concentration is approximately 13%.

As Eaton et al.,[11] Frey,[12] and Eaton[13] show, the CCD camera pixel values obtained when mapping the mixer flowfield are proportional to the number of fuel-stream seeding particles in the imaged sample volume. Consequently, the sum of all of the pixel values in an image is proportional to the total light intensity scattered from the fuel–air mixture in that sample. The input equivalence ratio ϕ can, therefore, be represented by the average pixel value obtained for an image encompassing the entire exit plane.

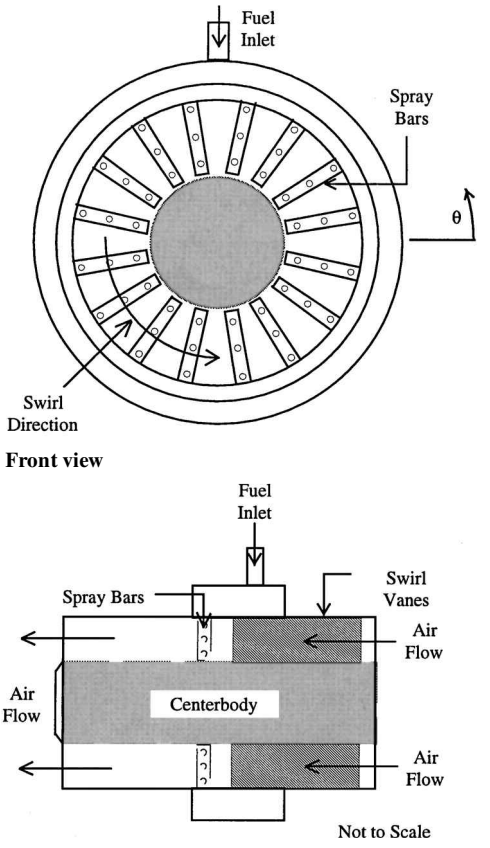

Fig. 1a Swirler schematic.[12]

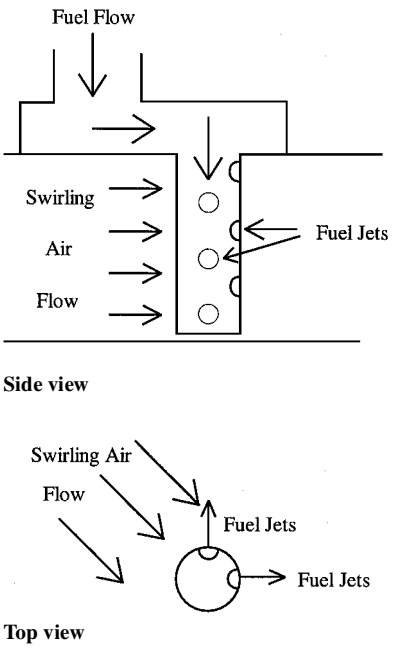

Fig. 1b Schematic of fuel jets in the swirling air flow.[13]

Data obtained during this study are presented in several different ways.[11] Typically, 25 instantaneous realizations were averaged to form a composite mixing image, from which spatial statistics were obtained. If pixel values throughout an image are normalized by the average pixel value for that image, a relative equivalence ratio ϕ_{rel} is obtained for each location in the premixer exit plane.

In general, the standard deviation of the recorded light intensity over the exit plane, evaluated about its average value, is

representative of the degree of mixing achieved. For instance, a perfectly mixed system would demonstrate the same scattered light intensity over the entire exit plane and a standard deviation of zero. We follow the methodology of Mikus and Heywood[14] and normalize the spatial standard deviation values by their corresponding averages to eliminate the effects of variable averages between realizations and to allow for direct comparison between all sets of data. This quotient is termed the unmixedness parameter s, for which lower values imply better mixing (a perfectly mixed case has a value of 0). Unmixedness parameter values for an entire image, or any subregion, can be calculated. Values of s were compared between cases to assess how changes in parameters influenced mixing.

III. Results

Baseline Case: Swirl Number of 1.1

A typical industrial gas-turbine premixer with swirl vanes set at an angle of 48 deg (swirl number of 1.1) was used as the baseline case. This geometry is close to the optimum configuration suggested both by the results of Ferrell et al.[3] and by the manufacturer's design testing.

Mixing information was obtained at the premixer exit plane for the baseline configuration. Two sets of 25 images were processed and averaged. The global s values for these two sets were 22 and 23%, respectively.[13]

The composite image was divided into 16 circumferential wedges (corresponding to the number of spray bars) and the s in each of these subregions was computed. Figure 2 shows the circumferential variation in s for the baseline cases (bases a and b), which are two entirely different runs. Note that the maximum unmixedness of approximately 24% occurs at $\theta = 80$ deg, whereas the minimum of approximately 14% occurs at $\theta = 180$ deg. The circumferential variations occur because the fuel was not distributed uniformly by the premixer plenum.

Radial variations in the relative equivalence ratio ϕ_{rel} were also observed, as shown in Fig. 3 and as discussed by Eaton.[13] Results for one of four diametral scans (the horizontal one) are presented in Fig. 3. The observed variations in fuel concentration result from a disproportionate amount of fuel being distributed closer to the centerbody.

Nonswirling Air Inlet Case

A modified premixer with straight vanes (as opposed to 48-deg swirl vanes) was tested to evaluate the influence (or absence) of swirl. Scalar concentration data were again acquired at the premixer exit plane. The results of three sets of data (25 images each) were compared to the baseline results.

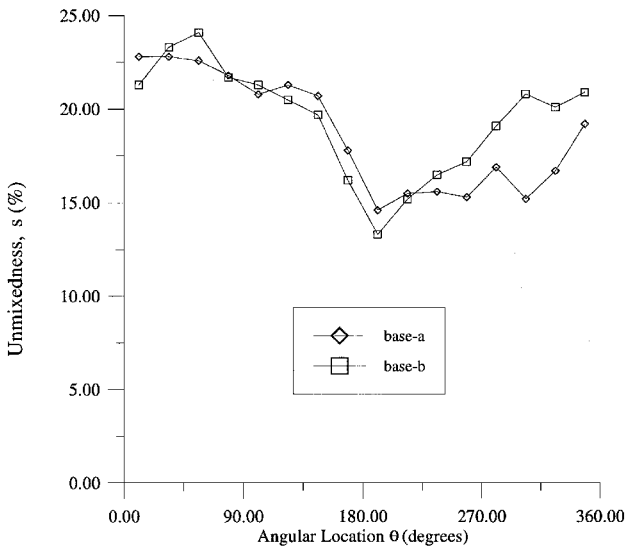

Fig. 2 Baseline unmixedness parameter s circumferential variation for a swirl number of 1.1; uncertainty in s (95% confidence) is 13%.

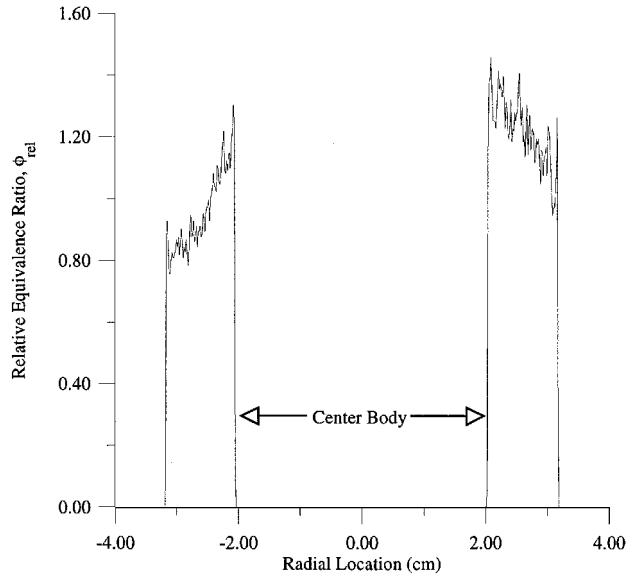

Fig. 3 Radial dependence of relative equivalence ratio ϕ_{rel} for the baseline case with a swirl number of 1.1; uncertainty in ϕ_{rel} (95% confidence) is 13%.

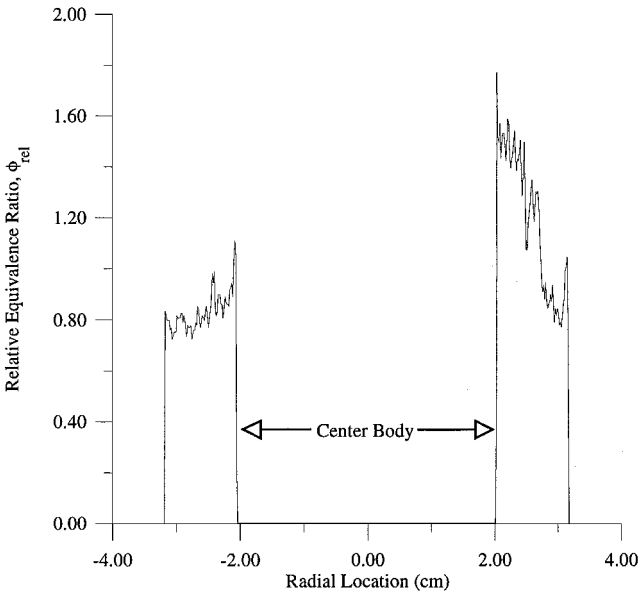

Fig. 4 Radial dependence of relative equivalence ratio ϕ_{rel} for the nonswirling case; uncertainty in ϕ_{rel} (95% confidence) is 13%.

Figure 4 contains an example ϕ_{rel} radial variation (the horizontal scan), similar to that presented in Fig. 3. It is representative of all radial scans in that it displays a considerable fuel concentration gradient from the centerbody to the outer rim. When compared to the baseline cases, the fractional radial variations in nonswirling ϕ_{rel} values are equal or greater, indicating worse mixing.

Unmixedness values for the baseline and nonswirling cases are provided in Fig. 5. Two features are noteworthy for the nonswirling cases. First, relatively fuel-rich regions are present at the top and bottom of the premixer. These locations are consistent with those observed for the swirling (baseline) case. That agreement has been enhanced by phase shifting the nonswirling data by an amount equal to the solid body rotation undergone by the flow in the swirling case.[13] Second, the baseline case has a lower s value in 12 of the 16 wedges.

The global exit plane values of s for the three sets of nonswirling data are 27, 26, and 23% with an average of 25% (Ref. 13). When compared to the baseline cases values of 22 and 23%, the nonswirling cases are somewhat less well mixed.

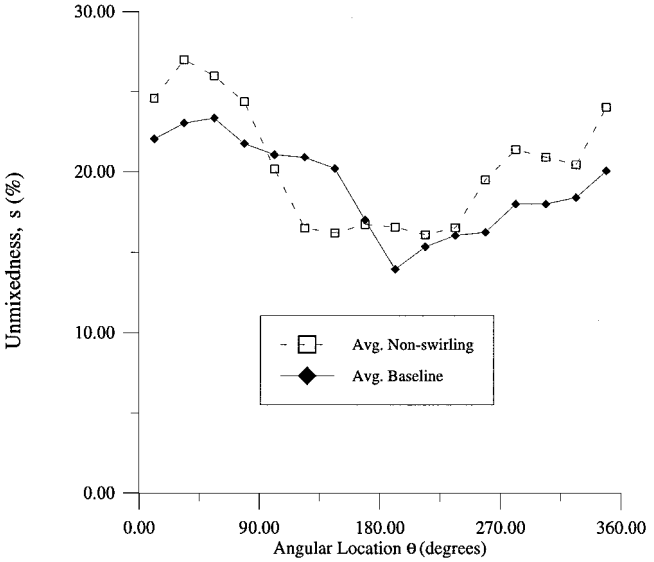

Fig. 5 Comparison of the baseline and phase shifted nonswirling average unmixedness parameter s vs angular location; uncertainty in s (95% confidence level) is 13%.

Data in Figs. 4 and 5, along with the global image s values, demonstrate that nonswirling cases were less well mixed than the swirling cases. The improved global mixing in the swirling case is partly attributed to the increased interaction time between the air and fuel in the premixer. Swirl also introduces additional strain rates that enhance turbulent mixing. The increased interaction time and enhanced turbulence might also account for the reduction in radial fuel concentration gradients. As the flow proceeds farther downstream, the jets are mixed with the crossflow and spread across a larger area due to diffusion and turbulent convection. If the jets and crossflow interact over a greater distance, the two fluids will become better mixed.

Comparisons to Literature

To put our study into perspective, we compare our results to recently reported work in swirling mixers utilizing entirely defferent experimental techniques. Mello et at.[15] and Barnes and Mellor[16] reported typical values of s of 10 to 30% at the exit of a similar premixer. Furthermore, they noted that s is a strong function of the mean premixer equivalence ratio.

Frazier et al.[17] report s values of 20% near the exit plane of dual-annular counter-rotating swirler–premixer. In addition, the overall equivalence ratio exhibited maximum spatial variations on the order of 50%.

IV. Discussion and Conclusions

Figures 2–5 present gas turbine premixer data, obtained using a planar imaging system, for both a baseline case with a swirl number of 1.1 and a nonswirling case. Data are presented in terms of the relative equivalence ratio ϕ_{rel} and standard deviation in the seeding particle scattered light intensity divided by the mean value, s parameter, in both angularly resolved and radial profile formats.

The baseline case exhibited fuel concentration nonuniformities, which included a global exit plane average s value of 22.5%. Premixer swirl vanes were replaced with three straight support vanes to eliminate the influence of swirl, with three observations being of interest.

First, circumferential and radial variations in mixing were observed in each case. Because the circumferential variations originate in the same location for both the swirling and nonswirling cases, we conclude that these variations arise from an asymmetrical distribution of fuel in the plenum.

Second, the overall unmixedness values for the swirling cases were lower than those for the nonswirling cases. The s parameter increased to an average of 25% for the three nonswirling cases. Thus, the introduction of swirl improved mixing as expected based on recent experimental and numerical studies. The improved mixing is attributed to the increased fuel–air interaction time in the premixer annulus.

Third, in cases where swirl and momentum ratio were examined concurrently,[13] the effects of swirl dominated the effects of momentum ratio. Therefore, mixing optimization should first focus on determining the optimum swirl angle (or range of angles) and then shift to an optimization of the momentum ratio.

In summary, these results suggest air and fuel mixing enhancements are achievable in actual gas turbine hardware operating at realistic flow rates by varying premixer swirl. Whereas further study of different swirl angle cases would provide useful information on the effects of swirl angle, the present results have demonstrated that swirl is an important parameter in the mixing process so an optimal range of swirl angles should exist. Further investigations are necessary to determine such an optimum.

Acknowledgment

The authors acknowledge the 1994 private communication from J. P. Gore concerning modifications to the reverse cyclone seeder.

References

[1]Favaloro, S. C., Nejad, A. S., and Ahmed, S. A., "Experimental and Computational Investigation of Isothermal Swirling Flow in an Axisymmetric Dump Combustor," *Journal of Propulsion and Power*, Vol. 7, No. 3, 1991, pp. 348–356.

[2]Halpin, J. L., "Swirl Generation and Recirculation Using Radial Swirl Vanes," American Society of Mechanical Engineers, ASME Paper 93-GT-169, June 1993.

[3]Ferrell, G. B., Aoki, K., and Lilley, D. G., "Flow Visualization of Lateral Jet Injection into Swirling Crossflows," AIAA Paper 85-0059, July 1985.

[4]Ong, L. H., McMurray, C. B., and Lilley, D. G., "Hot-Wire Measurements of a Single Lateral Jet Injected into Swirling Crossflow," AIAA Paper 86-0055, July 1986.

[5]Ahmed, S. A., and So, R. M. C., "Characteristics of Air Jets Discharging Normally into a Swirling Crossflow," *AIAA Journal*, Vol. 5, No. 3, 1987, pp. 429–435.

[6]Chao, Y. C., and Ho, W. C., "Heterogeneous and Nonisothermal Mixing of a Lateral Jet with a Swirling Crossflow," *Journal of Thermophysics*, Vol. 5, 1991, pp. 394–400.

[7]Chao, Y. C., and Ho, W. C.,"Numerical Investigations of Heated and Unheated Lateral Jets Discharging into a Confined Swirling Crossflow," *Numerical Heat Transfer, Part A*, Vol. 22, No. 3, 1992, pp. 343–361.

[8]Lilley, D. G., "Jet Penetration into Swirling Crossflows," *Proceedings of the 26th Intersociety Energy Conversion Engineering Conference,* Vol. 2, IEEE Pub., Piscataway, NJ, 1991, pp. 397–401.

[9]Lilley, D. G., "Vane Swirler Performance,"American Society of Mechanical Engineers, ASME Paper 95-GT-331, June 1995.

[10]Kounalakis, M. E., "Structure and Radiation Properties of Turbulent Diffusion Flames," Ph.D. Thesis, Dept. of Aerospace Engineering, Univ. of Michigan, Ann Arbor, MI, 1990.

[11]Eaton, A. R., Frey, S. F., Cusano, D. M., Plesniak, M. W., and Sojka, P. E., "Development of a Full-Field Planar Mie Scattering Technique for Evaluating Swirling Mixers," *Experiments in Fluids*, Vol. 21, No. 5, 1996, pp. 325–330.

[12]Frey, S. F., "Influence of Turbulence Characteristics and Premixer Length on the Performance of an Axial Swirl Premixer," M.S. Thesis, School of Mechanical Engineering, Purdue Univ., West Lafayette, IN, 1994.

[13]Eaton, A. R., "Influence of Air-to-Fuel Jet Momentum Ratio and Swirling Flow on the Performance of an Axial Swirl Premixer," M.S. Thesis, School of Mechanical Engineering, Purdue Univ., West Lafayette, IN, 1995.

[14]Mikus, T., and Heywood, J. B., "The Automotive Gas Turbine and Nitric Oxide Emissions," *Combustion Science and Technology,* Vol. 4, 1971, pp. 149–158.

[15]Mello, J. P., Mellor, A. M., Steele, R. C., and Smith, K. O., "A Study of the Factors Affecting NO_x Emissions in Lean Premixed Turbine Combustors," AIAA Paper 97-2708, July 1997.

[16]Barnes, J. C., and Mellor, A. M., "Quantifying Unmixedness in Lean Premixed Combustors Operating at High Pressure, Fired Condition," American Society of Mechanical Engineers, ASME Paper 97-GT-73, June 1997.

[17]Frazier, T. R., Foglesong, R. E., Coverdill, R. E., Peters, J. E., and Lucht, R. P., "An Experimental Investigation of Fuel/Air Mixing in an Optically Accessible Axial Premixer," AIAA Paper 98-3543, July 1998.